Journal of Molecular Graphics and Modelling 46 (2013) 59–64

Contents lists available at ScienceDirect

Journal of Molecular Graphics and Modelling

journal homepage: www.elsevier.com/locate/JMGM

Theoretical exploration to second-order nonlinear optical properties of new hybrid complexes via coordination interaction between (metallo)porphyrin and $[MSiW_{11}O_{39}]^{3-}$ (M = Nb^V or V^V) polyoxometalates

Ting Zhang, Nana Ma, Likai Yan*, Shizheng Wen, Tengying Ma, Zhongmin Su*

Institute of Functional Material Chemistry, Department of Chemistry, Northeast Normal University, Changchun 130024, People's Republic of China

ARTICLE INFO

Article history:
Accepted 25 September 2013
Available online 4 October 2013

Keywords:
Polyoxometalate
Pyridyl-porphyrin
Second-order nonlinear optical property
Density functional theory
π-Conjugation effect

ABSTRACT

The second-order nonlinear optical (NLO) properties of hybrid complexes via coordination interaction between porphyrin and Keggin-type polyoxometalates (POMs) α-$[MSiW_{11}O_{39}]^{3-}$ (M = Nb^V or V^V) are investigated by time-dependent density functional theory (TDDFT). The calculated results show that this kind of organic–inorganic hybrid complexes possesses remarkably large molecular second-order NLO polarizability, especially for the ZnP_3P-C≡C-4-Py-$[VSiW_{11}O_{39}]^{3-}$ (complex **4**), which has a computed β_0 value of 261,410 a.u. and might be an excellent second-order NLO material. The effects of substituted metal atom (M), metalloporphyrin, and π-conjugation on NLO response are analyzed, the substituted metal atom (M) with a large electronegativity, the metalloporphyrin, and the lengthening of π-conjugation are helpful in enhancing the optical nonlinearity of these systems, which reveal the general rules to design the complexes with large optical nonlinearities. Furthermore, the solvent effect largely affects the first-order hyperpolarizability of the complex, it implies that the second-order polarizabilities increased with the increase of the solvent in polarity.

1. Introduction

Organic–inorganic hybrids are a class of materials that integrate organic frameworks, inorganic clusters, and metal nodes in a framework structure. By incorporation of functional organic moieties and metal oxide clusters via self-assembly, grafting, or intercalation, such hybrid structures usually have multiple functionalities and new features as a result of blending of distinctively different components [1,2]. Within the context of nanostructured solids, the organic–inorganic hybrids provide a new pathway for combining multiple functional groups in a multilevel hierarchical framework at the molecular scale, which demonstrates the great potential for applications in diverse fields, such as selective adsorption, catalysis, explosives detection, optoelectronics, especially the NLO properties [3–7].

The NLO materials based on molecular compounds have continued to be of considerable current interest because they hold promise for potential applications in optical switching, telecommunications, optical computing, etc. [8–10]. And the organic–inorganic hybrid complexes may offer a greater scope for creation of multifunctional NLO materials by virtue of their low-energy, yet sometimes intense, electronic transitions.

Polyoxometalates (POMs), clusters of early transition metal cations bridged by oxide anions, have attracted particular attention in recent years because of their unique structures, highly tunable nature, and coupled with their fascinating properties, which lead to potential applications in materials science, biology, pharmacy, and NLO materials [11–14]. On the other hand, porphyrins are attractive components in materials because of their appealing chemical and photochemical properties: high stability, intense visible absorption bands, long-lived excited states, and tunability by chemical derivatization, and they are often used in supramolecular complexes [15–17].

Ruhlmann and co-workers have recently reported a new complex based on a coordination interaction between pyridyl-porphyrin and Keggin-type POM. And the formations of POM–porphyrin were assembled by axial coordination of POM-grafted pyridyl groups [18]. Based on the crystal of H_2P_3P-4-Py-$[MSiW_{11}O_{39}]^{6-}$ (M = Co^{II} and Ni^{II}, H_2P_3P-4-Py = 5,10,15-triphenyl-20-(4-pyridyl)porphyrin), we design a series of complexes H_2P_3P-4-Py-$[NbSiW_{11}O_{39}]^{3-}$, H_2P_3P-4-Py-$[VSiW_{11}O_{39}]^{3-}$, ZnP_3P-4-Py-$[VSiW_{11}O_{39}]^{3-}$, and ZnP_3P-C≡C-4-Py-$[VSiW_{11}O_{39}]^{3-}$. In this paper, our attention focuses on the POM-based organic derivatives as potential NLO

* Corresponding authors. Tel.: +86 431 85099108; fax: +86 431 85684009.
E-mail addresses: yanlk924@nenu.edu.cn (L. Yan), zmsu@nenu.edu.cn (Z. Su).

1093-3263/$ – see front matter © 2013 Elsevier Inc. All rights reserved.
http://dx.doi.org/10.1016/j.jmgm.2013.09.011

materials. We have investigated the second-order polarizabilities and origin of the NLO properties.

Over the past decade our group has systematically carried out the computational studies on Lindqvist, Keggin, Dawson, and related POM structures. The Density functional theory (DFT) approach has been shown to be appropriate to reproduce and explain their bonding character, redox properties, stability, IR spectra, and NLO properties [19–24]. Theoretical studies would be helpful in rationalization of the observed properties and design of novel POM-based hybrid materials with excellent properties. In this paper we focus on the connection between NLO properties and electrical characteristics, and the effect of solvation. To the best of our knowledge, this is the first theoretical characterization for these new complexes based on coordination interaction between pyridyl-porphyrin and Keggin-type POM.

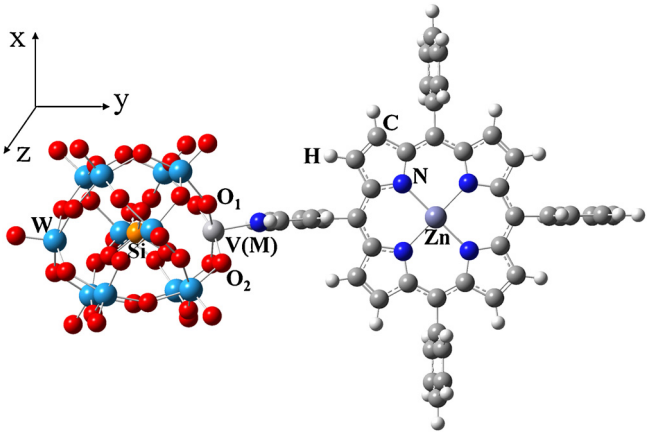

Fig. 1. Structure and orientation of complex **3**.

2. Computational details

The DFT calculations were carried out using the ADF2009.01 program [25]. Geometries of all complexes were optimized with C_s symmetry constraints. The local density approximation (LDA) characterized by the Vosko–Wilk–Nusair (VWN) parametrization for correlation was used [26]. The generalized-gradient approximation (GGA) was employed in the geometry optimizations by using the Beck and Perdew exchange-correlation (XC) functional [27,28]. The zero-order regular approximation (ZORA) was adopted in all the calculations to account for the scalar relativistic effects [29] with triple-ζ-plus-polarization quality (TZP) Slater-type orbital basis sets and incorporating frozen cores (V.2p, Zn.2p, Nb.3d, W.4d). All the geometries studied here by using the conductor-like screening model (COSMO) [30–32] to account for solvent effects ($C_2H_4Cl_2$, $\varepsilon = 10.66$), and the H_2P_3P-4-Py-$[NbSiW_{11}O_{39}]^{3-}$ (complex **1**) was optimized in CH_3Cl ($\varepsilon = 4.8$), CH_2Cl_2 ($\varepsilon = 8.9$) and CH_3CN ($\varepsilon = 37.5$) to examine the solvent effect on the NLO response. The suitable van der Waals radii are 1.08, 1.49, 1.40, 1.41, 2.10, 2.07, 2.07, 1.79 and 2.10 Å for H, C, O, N, W, Si, Nb, V and Zn [33]. Moreover, the value of the numerical integration parameter used to determine the precision of numerical integrals was 6.0.

The NLO coefficients of all complexes were calculated with the ADF-RESPONSE module based on the optimized geometries, and the statistical average of orbital potentials (SAOP) by Gritsenko and co-workers and Baerends and co-workers [34,35] was used.

In addition, to further interpret the charge transfer between organic group and POM, the natural bond orbital (NBO) calculation at the B3LYP level was performed using the GAUSSIAN 09W suite of programs [36], LanL2DZ basis set for W and V, Nb, Zn atoms and 6–31g(d) basis set for all non-metal elements were applied in this work.

3. Results and discussion

3.1. Molecular structures

Herein, four POM-(metallo)porphyrin compounds H_2P_3P-4-Py-$[NbSiW_{11}O_{39}]^{3-}$ (complex **1**), H_2P_3P-4-Py-$[VSiW_{11}O_{39}]^{3-}$ (complex **2**), ZnP_3P-4-Py-$[VSiW_{11}O_{39}]^{3-}$ (complex **3**), and ZnP_3P-C≡C-4-Py-$[VSiW_{11}O_{39}]^{3-}$ (complex **4**) were chosen for systematically investigating the second-order NLO properties. All complexes possess a similar geometrical structure with C_s symmetry. The structure of system 3 is shown in Fig. 1.

The main optimized bond distances of complexes **1**–**4** are listed in Table 1. It can be found that the bond distances of M—O_1, M—O_2, and M—N are obviously changed along with the replacement of M with Nb and V. For complexes **2**–**4**, the bond distances of M—O_1, M—O_2, and M—N are similar. And the other bond distances of all complexes are similar, so there's no obvious difference of structure between these complexes.

The main charge transfers of the porphyrin–polyoxometalate hybrids usually occur between porphyrin and POMs, and porphyrin has favorable conjugation, this is reminiscent of the distributed point charges used by Marder and collaborators in developing the bond-length alternation (BLA) scheme for nonlinear chromophores [37]. So we investigate the π conjugation of the porphyrin according to the bond distances. The term Δr is defined as the average difference between the bond lengths of two consecutive bonds in porphyrin. The porphyrin skeleton possesses inner and outer aromatic subfragments, as shown in Fig. 2, the bold lines in a and b stand for the inner and outer aromatic subfragments, respectively. According to the calculated electronic structure and X-ray crystallographic [38–40], the inner and outer aromatic subfragments have been proposed as chief porphyrin conjugative pathways. The BLA values of the inner and outer aromatic subfragments of all studied complexes have been listed in Table 1. The BLA values of complexes containing metalloporphyrin are smaller than complexes containing porphyrin. It indicates that the metal ions enhance the π conjugation. The BLA value is an important parameter that defines the NLO response for organic donor-π-acceptor molecules. For studied organic–inorganic hybrid polyoxoanions, the complex with larger BLA value might display larger static second-order polarizabilities.

The natural bond orbital (NBO) charge distribution of organic group and heteropolyanion were calculated to predict the possible charge transfer. The NBO charge transfers of complexes **1**–**4** from organic group to heteropolyanion are 0.31, 0.41, 0.41 and 0.42e$^-$, respectively. The NBO charge transfer of complex **1** is the minimum of these complexes, while the charge transfers of complexes **2**–**4** are similar and larger than complex **1**. Thus, the charge transfer between organic group and heteropolyanion cluster is increased when the substituted metal M is V. The result indicates that the NBO charge transfer is closely related to the electronegativity of the substituted metal atom (M). As the electronegativity of atom V

Table 1
The optimized bond distances of complexes **1**–**4** and the bond length alternation values, Δr, of inner and outer aromatic subfragments of porphyrin ring (Å).

	Complex			
	1	**2**	**3**	**4**
M—O_1	1.93	1.76	1.76	1.76
M—O_2	1.97	1.90	1.90	1.90
M—N	2.18	2.05	2.05	2.03
Δr (inner)	0.024	0.024	0.019	0.021
Δr (outer)	0.028	0.028	0.029	0.029

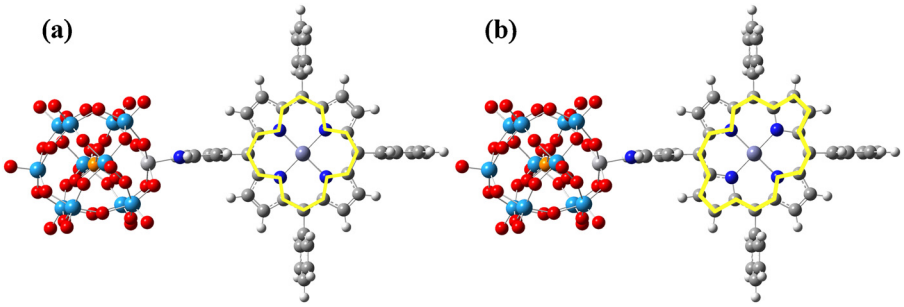

Fig. 2. (a and b) The inner and outer aromatic subfragments of the porphyrin skeleton.

is larger than that of Nb, the ability of obtaining electron for V is better than that of Nb.

3.2. Spectrum properties

To get more insights of the main charge transfer for these complexes, we have performed time-dependent density functional theory (TDDFT) calculations to obtain electronic spectra. The calculated transition energies, vertical transition wavelengths, oscillator strength, and dominant molecular orbital (MO) transitions of complexes **1**–**4** are summarized in Table 2. The MOs involved in the dominant electron transitions in studied complexes are shown in Fig. 3. For complex **1**, the transition is mainly generated from HOMO to LUMO+8, and from HOMO-1, HOMO-3 to LUMO+7. It can be seen that charge transfer mainly occurs $\pi \rightarrow \pi^*$ within the porphyrin along the *y*-axis. The electron transition of complex **2** mainly arises from HOMO-20, HOMO-22 to LUMO+1, and from HOMO to LUMO+27 along the *y*-direction, the occupied orbitals involved in the electronic transitions mainly delocalize over the π orbitals of porphyrin, and p orbitals of oxygen atoms in POM, whereas the unoccupied orbitals are d orbitals of vanadium and a few p orbitals of oxygen in polyoxometalates. For complex **3**, the electron transition is mainly from HOMO-27, HOMO-18 to LUMO+1, the characteristic of the unoccupied orbitals for complex **3** are similar to those of complex **2**, and the occupied orbitals are p orbitals of carbon atoms and nitrogen atoms. The electron transitions of complex **4** are generated by the promotion of electrons from HOMO-14 to LUMO+1 and from HOMO to LUMO+8. For the first electron transition, the unoccupied orbitals are also similar to those of complex **2**, and the occupied orbitals are p orbitals of carbon atoms in the benzene ring, whereas the other electron transition characteristic from HOMO to LUMO+8 is similar to complex **1**. These behaviors indicate that the organic groups of complexes **2**–**4** act as the donor and the POMs act as the acceptor. In addition, it can be found from Table 2, λ_{gm} values are related to the charge transfer character of the studied complexes, and λ_{gm} values increase from complexes **1** to **4**. The λ_{gm} value of complex **1** is only 419 nm, whereas for complex **4**, the maximum wavelength of the absorption band is 632 nm. Clearly, the absorption bands possess remarkably bathochromic shift from complexes **1** to **4**.

In our previous work [41], The NLO properties of sandwich type porphyrin–metal–polyoxometalate (por–metal–POM) compounds in which a group IV transition metal ion (Hf and Zr) coordinates a porphyrin and a lacunary defect in a Keggin were investigated. The porphyrin ligand acts as an electron donor and the lacunary POM cluster acts as an electron acceptor. In this work, the main charge transfers of systems **2**–**4** are from carbon and nitrogen atoms to vanadium and oxygen atoms in polyoxometalates. These behaviors indicate that the organic groups of complexes **2**–**4** act as the donor and the POMs act as the acceptor.

3.3. The static second-order polarizability

The static second-order polarizability (β_0) is termed the zero-frequency hyperpolarizability and is an estimate of intrinsic molecular hyperpolarizability in the absence of any resonance effects. The static second-order polarizability, β_0, was calculated by using the following equation (Eq. (1)):

$$\beta_0 = (\beta_x^2 + \beta_y^2 + \beta_z^2)^{1/2} \quad (1)$$

where β_x, β_y and β_z are the components of the second-order polarizability tensor along the *x*-, *y*- and *z*-axis, respectively, and β_i can be expressed as the equation (Eq. (2)):

$$\beta_i = \frac{3}{5} \sum_{j=x,y,z} \beta_{ijj} \quad (2)$$

The computed individual components of β_0 values in complexes **1**–**4** are shown in Table 3. There are 14 nonzero components of second-order polarizability owing to C_s symmetry, but only six tensor components are independent ($\beta_{yzz} = \beta_{zyz} = \beta_{zzy}$, $\beta_{xzz} = \beta_{zxz} = \beta_{zzx}$, $\beta_{xyy} = \beta_{yxy} = \beta_{yyx}$, $\beta_{xxy} = \beta_{xyx} = \beta_{yxx}$). From Table 3, it can be seen that β_{yyy} component has the largest value. Hence, β_{yyy} component is the major contribution to the second-order polarizability and the charge transfer direction of all complexes lies in the *y*-axis (see

Table 2
Transition energy ΔE_{gm} (eV), transition wavelengths (λ_{gm}, nm), oscillator strength (*f*), and the corresponding dominant MO transitions for complexes **1**–**4**.

Complex	ΔE_{gm}	λ_{gm}	f_{gm}	MO transition
1	2.95	419	0.2771	HOMO → LUMO+8 (25%) HOMO-3 → LUMO+7 (13%) HOMO-1 → LUMO+7 (12%)
2	2.86	433	0.1887	HOMO-22 → LUMO+1 (31%) HOMO-20 → LUMO+1 (28%) HOMO → LUMO+27 (24%)
3	2.80	441	0.1641	HOMO-18 → LUMO+1 (78%) HOMO-27 → LUMO+1 (6%)
4	1.96	632	0.4988	HOMO-14 → LUMO+1 (91%) HOMO → LUMO+8 (91%)

Table 3
The calculated individual components of second-order polarizabilities, and β_0 values of complexes **1**–**4** (a.u.).

	Complex			
	1	**2**	**3**	**4**
β_{yyy}	−11,220	−40,855	−10,3450	−21,8910
β_{xyy}	−313	1177	2032	5123
β_{yzz}	93	299	302	330
β_{xzz}	99	120	119	122
β_{xxx}	1	55	66	80
β_{xxy}	63	15	2	135
β_0	13,278	48,552	123,570	261,410

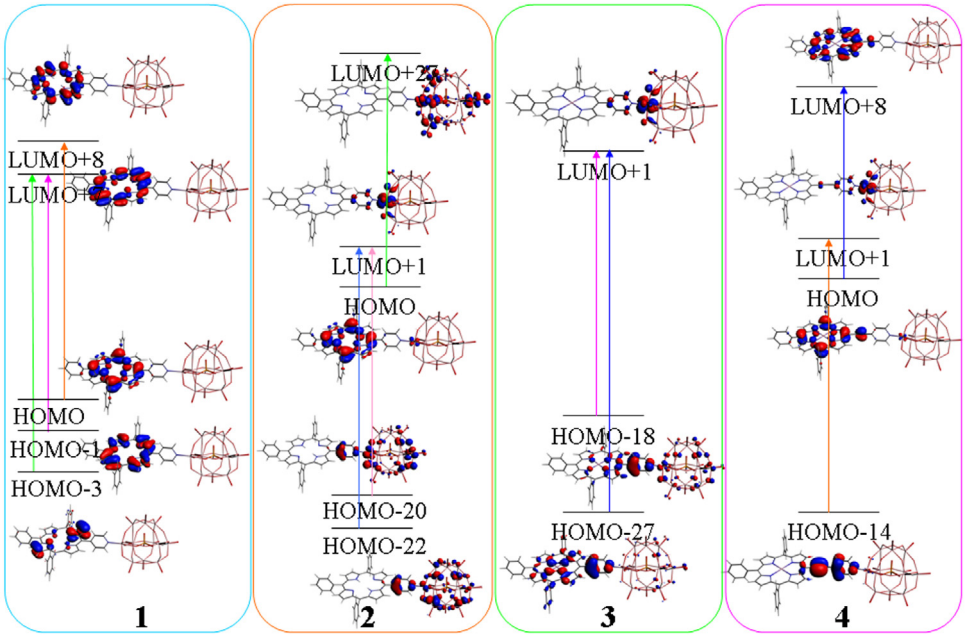

Fig. 3. Molecular orbital diagram for complexes **1**–**4** involved in the dominant electron transitions.

Fig. 3), which further confirm the charge transfer character discussed above.

From the chemical standpoint, the most important feature of the NLO theoretical calculations could provide the effect of subtle variations on NLO properties. In order to understand the NLO response of these POM–(metallo)porphyrin complexes, three aspects are chosen to probe the substituent effects on the second-order polarizability, including the substituted metal atom (M), metalloporphyrin, and the π-conjugation effects. From Table 3, it can be seen that the β_0 value of complex **2** is larger than that of complex **1**. It indicates that the second-order polarizability is sensitive to the substituted metal atom. It can be explained from the character of charge transfer transition. For complex **1** with substituted metal Nb, the major charge transition mainly occurs $\pi \rightarrow \pi^*$ within the porphyrin along the *y*-axis. While in complex **2** with substituted metal V, the charge transfer transition mainly occurs between the POMs and the organic group, which is different from the charge transfer of complex **1**. The β_0 value of complex **3** is 123,570 a.u., which is larger than that of complex **2** (48,552 a.u.). It can be associated with the enhanced π conjugated of metalloporphyrin, and the β_0 values are in good agreement with the variation tendency of the BLA values. The β_0 value for complex **4** is 261,410 a.u., which is close to two times as large as that of complex **3**. The complex **4** is lengthened via —C≡C— with respect to complex **3**, thus, the π-conjugation is extended and the delocalization is improved. More extended conjugation generally leads to a smaller energy difference between the ground and excited states, which enhances the degree of charge transfer. It can be concluded that the increase of the π-conjugation effects and the charge transfer from the organic group to POMs are helpful in enhancing the β_0 values. In summary, the promising NLO response can be enhanced by subtle variation in the molecular architecture. In addition, all studied complexes have large second-order polarizability coefficients, especially for complex **4**, which charge transfer occurs between POM and porphyrin. It indicates that these complexes have a great potential in excellent second-order NLO response.

To shed light on the origin of the second-order NLO performance of studied polyanions, the elucidation of the structure–property relationship is necessary. A simple link between β_0 and electronic transition (*s*) in low-lying crucial excited states have been established from the sum-over-states (SOS) expression by Oudar and Chemla [42,43]. For the static case ($\omega = 0.0$), the following two-level expression is employed to estimate β_0 (Eq. (3)):

$$\beta_0 \propto \frac{\Delta\mu_{gm} f_{gm}}{E_{gm}^3} \tag{3}$$

where f_{gm}, E_{gm}, and $\Delta\mu_{gm}$ are the oscillator strength, transition energy, and the difference of the dipole moment between the ground state (*g*) and the *m*th excited state (*m*), respectively. In the two-state model expression, the second-order polarizability caused by charge transfer, β_0, is proportional to the optical intensity and the dipole moment between the ground state (*g*) and the *m*th excited state (*m*), and is inversely proportional to the cube of the transition energy. Hence, the transition energy is a decisive factor in the β_0 value.

As can be seen from Table 2, the transition energies of complexes **1**, **2** and **3** are 2.95, 2.86 and 2.80 eV, respectively. According to Eq. (3), smaller transition energy is helpful for larger β_0 value, and the computed β_0 values of complexes **1**–**3** increase as follows: 1 < 2 < 3. The complex **4** with the smallest transition energy and the largest oscillator strength presents the largest β_0 value, 261,410 a.u., which is two times as large as that of complex **3**.

3.4. Effect of solvation on NLO response

In general, the polarity of solvent is said to affect NLO properties [44,45]. Therefore we calculate the β_0 value of complex **1** in different solvents with varying polarity to study the solvent effect on NLO property. The second-order polarizabilities are calculated in the presence of solvents such as chloroform, dichloromethane, dichloroethane, acetonitrile, and the results are summarized in Table 4. It implies that the second-order polarizabilities increased with the increase of the solvent in polarity $CHCl_3 < CH_2Cl < C_2H_4Cl_2 < CH_3CN$. Thus, the solvent polarity obviously affects NLO property of the POM–porphyrin complex. This can be attributed to the strong polarity improving the obvious charge-separated [46].

The functionals for evaluating the β_{tot} values are usually general gradient approximation (GGA) in recent years. Moreover, the Hartree–Fock (HF) exchange function and long-range function can

Table 4
Effect of solvent polarity on second-order polarizabilities for complexes **1** (a.u.).

	Solvent			
	$CHCl_3$	CH_2Cl_2	$C_2H_4Cl_2$	CH_3CN
SAOP	8415	11,785	13,278	19,420
M06-2X	6896	7881	8022	8827
CAM-B3LYP	6732	7665	7798	8554

be included to obtain more reasonable results. Thus, two types of density functional were selected in this study to examine the reliability of the calculated results. We used the meta-GGA M06-2X functional which includes a high percentage of HF exchange and CAM-B3LYP including long range corrections to calculate the β values by using the GAUSSIAN 09W suite of programs [36], LanL2DZ basis set for W and Nb atoms and 6–31g(d) basis set for all non-metal elements were applied in this work. We calculated the hyperpolarizabilities of complex **1** in different solvents, and the results are summarized in Table 4. Comparing with the result of calculating with SAOP, it implies that the second-order polarizabilities also increase with the increase of solvent polarity $CH_3Cl < CH_2Cl < C_2H_4Cl_2 < CH_3CN$. Although the calculated values complex are not same by different functionals, while, the trends are all the same.

4. Conclusions

In this paper, the static second-order NLO responses of a series of hybrid complexes via coordination interaction between porphyrin and α-$[MSiW_{11}O_{39}]^{3-}$ ($M = Nb^V$ or V^V), were investigated based on systematic DFT calculations. The effects of the substituted metal atom (M), metalloporphyrin, and π-conjugation on the NLO response are analyzed and the computed β_0 values as well as the structure-property relationship indicate that there are three ways to enhance the NLO response of this class of organic–inorganic hybrid complexes. (1) First, the substituted metal atom (M) with a large electronegativity (V > Nb) have a larger nonlinearity. (2) The metalloporphyrin enhances the π-conjugation effect and is helpful in enhancing the optical nonlinearity of complexes **3** and **4**. (3) Third, the lengthening of π-conjugation is helpful for larger optical nonlinearity. Furthermore, the solvent effect largely affects the second-order polarizability of the complex. It is expected that the results presented in this work will stimulate experimental research in the field of NLO materials involving the organic–inorganic hybrid structure based on porphyrin and POM.

Acknowledgments

The authors gratefully acknowledge financial support by NSFC (21073030 and 21131001), Program for New Century Excellent Talents in University (NCET-10-318), Doctoral Fund of Ministry of Education of China (20100043120007), and the Science and Technology Development Planning of Jilin Province (20100104, 20100320).

References

[1] M.J. Rosseinsky, Recent developments in metal–organic framework chemistry: design, discovery, permanent porosity and flexibility, Microporous Mesoporous Mater. 73 (2004) 15–30.
[2] A.K. Cheetham, C.N.R. Rao, R.K. Feller, Structural diversity and chemical trends in hybrid inorganic–organic framework materials, Chem. Commun. (2006) 4780–4795.
[3] A.J. Lan, K.H. Li, H.H. Wu, D.H. Olson, T.J. Emge, W. Ki, M.C. Hong, J. Li, A luminescent microporous metal–organic framework for the fast and reversible detection of high explosives, Angew. Chem. Int. Ed. 48 (2009) 2334–2338.
[4] Y. El-Nahal, S. Nir, C. Serban, O. Rabinovitch, B. Rubin, Montmorillonite-phenyltrimethylammonium yields environmentally improved formulations of hydrophobic herbicides, J. Agric. Food Chem. 48 (2000) 4791–4801.
[5] E. Ruiz-Hitzky, Molecular access to intracrystalline tunnels of sepiolite, J. Mater. Chem. 11 (2001) 86–91.
[6] H. Wellmann, J. Rathousky, M. Wark, A. Zukal, G. Schulz-Ekloff, Formation of CdS nanoparticles within functionalized siliceous MCM-41, Microporous Mesoporous Mater. 44 (2001) 419–425.
[7] S. Pramanik, C. Zheng, T.J. Emge, J. Li, New microporous metal–organic framework demonstrating unique selectivity for detection of high explosives and aromatic compounds, J. Am. Chem. Soc. 133 (2011) 4153–4155.
[8] J.J. Wang, Z.J. Zhou, Y. Bai, Z.B. Liu, Y. Li, D. Wu, W. Chen, Z.R. Li, C.C. Sun, The interaction between superalkalis (M_3O, M = Na, K) and a $C_{20}F_{20}$ cage forming superalkali electride salt molecules with excess electrons inside the $C_{20}F_{20}$ cage: dramatic superalkali effect on the nonlinear optical property, J. Mater. Chem. 22 (2012) 9652–9657.
[9] C. Huang, C.L. Hu, X. Xu, B.P. Yang, J.G. Mao, $Tl(VO)_2O_2(IO_3)_3$: a new polar material with a strong SHG response, Dalton Trans. 42 (2013) 7051–7058.
[10] C.G. Liu, X.H. Guan, Computational study on redox-switchable second-order nonlinear optical properties of totally inorganic Keggin-type polyoxometalate complexes, J. Phys. Chem. C 117 (2013) 7776–7783.
[11] T. Akutagawa, D. Endo, S.I. Noro, L. Cronin, T. Nakamura, Directing organic–inorganic hybrid molecular-assemblies of polyoxometalate crown-ether complexes with supramolecular cations, Coord. Chem. Rev. 251 (2007) 2547–2561.
[12] D.L. Long, R. Tsunashima, L. Cronin, Polyoxometalates: building blocks for functional nanoscale systems, Angew. Chem. Int. Ed. 49 (2010) 1736–1758.
[13] N. Mizuno, K. Yamaguchi, K. Kamata, Epoxidation of olefins with hydrogen peroxide catalyzed by polyoxometalates, Coord. Chem. Rev. 249 (2005) 1944–1956.
[14] P. Kögerler, B. Tsukerblat, A. Müller, Structure-related frustrated magnetism of nanosized polyoxometalates: aesthetics and properties in harmony, Dalton Trans. 39 (2010) 21–36.
[15] F. Scandola, C. Chiorboli, A. Prodi, E. Iengo, E. Alessio, Photophysical properties of metal-mediated assemblies of porphyrins, Coord. Chem. Rev. 250 (2006) 1471–1496.
[16] H. Imahori, S. Fukuzumi, Porphyrin- and fullerene-based molecular photovoltaic devices, Adv. Funct. Mater. 14 (2004) 525–536.
[17] D. Hagrman, P.J. Hagrman, J. Zubieta, Solid-state coordination chemistry: the self-assembly of microporous organic–inorganic hybrid frameworks constructed from tetrapyridylporphyrin and bimetallic oxide chains or oxide clusters, Angew. Chem. Int. Ed. 38 (1999) 3165–3168.
[18] D. Schaming, C. Costa-Coquelard, I. Lampre, S. Sorgues, M. Erard, X. Liu, J. Liu, L. Sun, J. Canny, R. Thouvenot, L. Ruhlmann, Formation of a new hybrid complex via coordination interaction between 5,10,15-tritolyl-20-(4-and3-pyridyl)porphyrin or 5,10,15-triphenyl-20-(4-pyridyl)porphyrin and the α-$[MSiW_{11}O_{39}]^{6-}$ Keggin-type polyoxometalate ($M = Co^{2+}$ and Ni^{2+}), Inorg. Chim. Acta 363 (2010) 2185–2192.
[19] L.K. Yan, X. López, J.J. Carbó, R. Sniatynsky, D.C. Duncan, J.M. Poblet, On the origin of alternating bond distortions and the emergence of chirality in polyoxometalate anions, J. Am. Chem. Soc. 130 (2008) 8223–8233.
[20] N.N. Ma, L.K. Yan, W. Guan, Y.Q. Qiu, Z.M. Su, Theoretical investigation on electronic structure and second-order nonlinear optical properties of novel hexamolybdate-organoimido-(car)borane hybrid, Phys. Chem. Chem. Phys. 14 (2012) 5605–5612.
[21] T. Zhang, N.N. Ma, L.K. Yan, S.Z. Wen, Z.M. Su, Theoretical exploration to the substituting effect on second-order nonlinear optical properties for lacunary γ-Keggin polyoxometalates, Chem. Phys. Lett. 557 (2013) 123–128.
[22] J.P. Wang, L.K. Yan, W. Guan, S.Z. Wen, Z.M. Su, The structure–property relationship of chiral 1,1′-binaphthyl-based polyoxometalates: TDDFT studies on the static first hyperpolarizabilities and the ECD spectra, J. Mol. Graph. Modell. 32 (2012) 1–8.
[23] S.Z. Wen, W. Guan, L.K. Yan, Z.M. Su, S. Sanvitob, First principle investigation of transport properties of Lindqvist derivatives based molecular junction, J. Mol. Graph. Modell. 38 (2012) 220–225.
[24] T.Y. Ma, N.N. Ma, L.K. Yan, W. Guan, Z.M. Su, Theoretical studies on the photoisomerization-switchable second-order nonlinear optical responses of DTE-linked polyoxometalate derivatives, J. Mol. Graph. Modell. 40 (2013) 110–115.
[25] ADF2009.01, SCM, Theoretical Chemistry, Vrije Universiteit, Amsterdam, The Netherlands, 2009, Available at: http://www.scm.com
[26] S.H. Vosko, L. Wilk, M. Nusair, Accurate spin-dependent electron liquid correlation energies for local spin density calculations: a critical analysis, Can. J. Phys. 58 (1980) 1200–1211.
[27] A.D. Becke, Density-functional exchange-energy approximation with correct asymptotic behavior, Phys. Rev. A 38 (1988) 3098–3100.
[28] J.P. Perdew, Density-functional approximation for the correlation energy of the inhomogeneous electron gas, Phys. Rev. B 33 (1986) 8822–8824.
[29] E. van Lenthe, E.J. Baerends, J.G. Snijders, Relativistic regular two-component Hamiltonians, J. Chem. Phys. 99 (1993) 4597–4610.
[30] E. van Lenthe, A.E. Ehlers, E.J. Baerends, Geometry optimizations in the zero order regular approximation for relativistic effects, J. Chem. Phys. 110 (1999) 8943–8953.
[31] A. Klamt, Conductor-like screening model for real solvents: a new approach to the quantitative calculation of solvation phenomena, J. Phys. Chem. 99 (1995) 2224–2235.

[32] A. Klamt, V. Jones, Treatment of the outlying charge in continuum solvation models, J. Chem. Phys. 105 (1996) 9972–9981.
[33] S.Z. Hu, Z.H. Zhou, K.R. Tsai, Average van der Waals radii of atoms in crystals, Acta. Phys. Chim. Sin. 19 (2003) 1073–1077.
[34] S.J.A. van Gisbergen, J.G. Snijders, E.J. Baerends, Implementation of time-dependent density functional response equations, Comput. Phys. 118 (1999) 119–138.
[35] P.R.T. Schipper, O.V.S. Gritsenko, J.A. Gisbergen, E.J. Baerends, Molecular calculations of excitation energies and (hyper)polarizabilities with a statistical average of orbital model exchange-correlation potentials, J. Chem. Phys. 112 (2000) 1344–1352.
[36] M.J. Frisch, G.W. Trucks, H.B. Schlegel, G.E. Scuseria, M.A. Robb, J.R. Cheeseman, G. Scalmani, V. Barone, B. Mennucci, G.A. Petersson, H. Nakatsuji, M. Caricato, X. Li, H.P. Hratchian, A.F. Izmaylov, J. Bloino, G. Zheng, J.L. Sonnenberg, M. Hada, M. Ehara, K. Toyota, R. Fukuda, J. Hasegawa, M. Ishida, T. Nakajima, Y. Honda, O. Kitao, H. Nakai, T. Vreven, J.A. Montgomery Jr., J.E. Peralta, F. Ogliaro, M. Bearpark, J.J. Heyd, E. Brothers, K.N. Kudin, V.N. Staroverov, R. Kobayashi, J. Normand, K. Raghavachari, A. Rendell, J.C. Burant, S.S. Iyengar, J. Tomasi, M. Cossi, N. Rega, J.M. Millam, M. Klene, J.E. Knox, J.B. Cross, V. Bakken, C. Adamo, J. Jaramillo, R. Gomperts, R.E. Stratmann, O. Yazyev, A.J. Austin, R. Cammi, C. Pomelli, J.W. Ochterski, R.L. Martin, K. Morokuma, V.G. Zakrzewski, G.A. Voth, P. Salvador, J.J. Dannenberg, S. Dapprich, A.D. Daniels, O. Farkas, J.B. Foresman, J.V. Ortiz, J. Cioslowski, D.J. Fox, Gaussian 09W Revision A, 02, Gaussian, Inc., Wallingford, CT, 2009.
[37] F. Meyers, S.R. Marder, B.M. Pierce, J.L. Bredas, Electric field modulated nonlinear optical properties of donor–acceptor polyenes: sum-over-states investigation of the relationship between molecular polarizabilities (.alpha.,.beta., and.gamma.) and bond length alternation, J. Am. Chem. Soc. 116 (1994) 10703–10714.
[38] M. Gouterman, G. Wagmere, Spectra of porphyrins: Part II. Four orbital model, J. Mol. Spectrosc. 11 (1963) 108–127.
[39] C. Weiss, H. Kobayashi, M. Gouterman, Spectra of porphyrins: Part III. Self-consistent molecular orbital calculations of porphyrin and related ring systems, J. Mol. Spectrosc. 16 (1963) 415–450.
[40] J.H. Fuhrhop, The reactivity of the porphyrin ligand, Angew. Chem. Int. Ed. 13 (1974) 321–335.
[41] C. Yao, L.K. Yan, W. Guan, C.G. Liu, P. Song, Z.M. Su, Prediction of second-order optical nonlinearity of porphyrin–metal–polyoxometalate sandwich compounds, Dalton Trans. 39 (2010) 7645–7649.
[42] J.L. Oudar, D.S. Chemla, Hyperpolarizabilities of the nitroanilines and their relations to the excited state dipole moment, J. Chem. Phys. 66 (1977) 2664–2668.
[43] J.L. Oudar, Optical nonlinearities of conjugated molecules. Stilbene derivatives and highly polar aromatic compounds, J. Chem. Phys. 67 (1977) 446–457.
[44] R. Cammi, B. Mennucci, J. Tomasi, Solvent effects on linear and nonlinear optical properties of donor–acceptor polyenes: investigation of electronic and vibrational components in terms of structure and charge distribution changes, J. Am. Chem. Soc. 120 (1998) 8834–8847.
[45] Y. Yamaguchi, Y. Yokomichi, S. Yokoyama, S. Mashiko, Theoretical study of solvent effects of first-order hyperpolarizabilities of nitro-azobenzene dendrimers, J. Mol. Struct. THEOCHEM 578 (2002) 35–45.
[46] R. Vijay Solomon, P. Veerapandian, S. Angeline Vedha, P. Venuvanalingam, Tuning nonlinear optical and optoelectronic properties of vinyl coupled triazene chromophores: a density functional theory and time-dependent density functional theory investigation, J. Phys. Chem. A 116 (2012) 4667–4677.